A Highly Stable Zeotype Mesoporous Zirconium Metal–Organic Framework with Ultralarge Pores**

Dawei Feng, Kecheng Wang, Jie Su, Tian-Fu Liu, Jihye Park, Zhangwen Wei, Mathieu Bosch, Andrey Yakovenko, Xiaodong Zou, and Hong-Cai Zhou

Abstract: *Through topological rationalization, a zeotype mesoporous Zr-containing metal–organic framework (MOF), namely PCN-777, has been designed and synthesized. PCN-777 exhibits the largest cage size of 3.8 nm and the highest pore volume of 2.8 cm³ g⁻¹ among reported Zr-MOFs. Moreover, PCN-777 shows excellent stability in aqueous environments, which makes it an ideal candidate as a support to incorporate different functional moieties. Through facile internal surface modification, the interaction between PCN-777 and different guests can be varied to realize efficient immobilization.*

Mesoporous metal-organic frameworks (MOFs) have been extensively studied as heterogeneous platforms to immobilize functional moieties, such as organometallic catalysts, nanoparticles, polyalkyl amine chains, and enzymes.[1,2] As a result of their readily adjustable structures and tunable functionalities inside the frameworks, mesoporous MOFs facilitate the performance of those materials through heterogenization or isolation. However, the majority of reported MOFs are microporous. Difficulty in the extension of organic linkers,

[*] D. Feng,[+] K. Wang,[+] Dr. T.-F. Liu, J. Park, Dr. Z. Wei, M. Bosch, Prof. Dr. H.-C. Zhou
Department of Chemistry, Texas A& M University
College Station, TX 77843 (USA)
E-mail: zhou@chem.tamu.edu
Homepage: http://www.chem.tamu.edu/rgroup/zhou/

Dr. J. Su, Prof. Dr. X. Zou
Berzelii Center EXSELENT on Porous Materials and
Inorganic and Structural Chemistry
Department of Materials and Environmental Chemistry
Stockholm University, 10691 Stockholm (Sweden)

Dr. A. Yakovenko
X-ray Science Division, Advanced Photon Source
Argonne National Laboratory, Argonne, IL 60439 (USA)

[+] These authors contributed equally to this work.

Supporting information for this article is available on the WWW under http://dx.doi.org/10.1002/anie.201409334.

variation of synthetic conditions in isoreticular structures, framework interpenetration, and challenges in activation all hamper the development of novel mesoporous MOFs. Most importantly, when the size of the organic linker increases, both the mechanical and the chemical stability of the framework decrease gradually.[3] Furthermore, the working environments of those immobilized moieties are usually harsh, which requires the frameworks to be chemically very stable. The requirement of a combination of good chemical stability and a large pore size means that very few candidates are widely utilized. MIL-101 (MIL: Materials of Institut Lavoisier) and MIL-100 are two extraordinary examples that exhibit both properties and can be used as suitable supports.[4]

MIL-100 and MIL-101, both of which have zeotype **mtn** topology (zeotype refers to structures sharing the same topology as zeolites), contain super-tetrahedral cages to substitute for the tetrahedral unit in zeolites.[5] Thus, their largest pores reach 31 Å and 29 Å, respectively, although the organic linkers are relatively small. Moreover, the metal nodes in these MOFs are based on trivalent metal species. The strong interaction between carboxylates and high-valent metal species accompanied with the small organic linker endows these frameworks with excellent chemical stability.

Despite these advantages, the pore size still restricts further application of these MOFs when it comes to larger guests, such as nanoparticles or enzymes. Therefore, synthesis of mesoporous materials with larger pore sizes which also maintain excellent chemical stability is highly desired. The use of a larger ligand than those employed in the MIL-100 and MIL-101 MOFs to create zeotype frameworks would be an effective way to generate extra-large pores, while avoiding a complicated organic synthetic route to make very large linkers. Unfortunately, several challenges must be addressed to extend the series of **mtn** topological MOFs: a) the $[M_3O(COO)_6]$ building block (M = Fe^{III}, Al^{III}, Cr^{III}, In^{III}, V^{III}, Sc^{III}) is not the thermodynamically favored form, which makes the controllable formation of target products difficult,[6] b) even if the inorganic building block can be obtained, competitive framework isomers, such as the MIL-88 structure,[6d] still dominate as the major products, and c) most of the synthesis should be conducted under hydrothermal conditions, which is infeasible for large organic linkers with poor water solubility. Therefore, searching for other zeotype frameworks, which can be more easily synthetically controlled, is one promising strategy.

Through a topological analysis, we present herein a zeotype mesoporous Zr-MOF, namely PCN-777, which has a β-cristobalite-type structure (PCN = porous coordination net-

work). PCN-777 exhibits the largest cage (3.8 nm) and the highest porosity (2.8 cm³ g⁻¹) among reported Zr-MOFs. Moreover, it shows high stability in aqueous solution over a wide range of pH values.

Zirconium MOFs have been extensively studied recently as a result of their excellent chemical stability.[7] One major reason is the controllable synthesis of crystalline products or even single crystals by using competing reagents.[8] Moreover, a Zr_6 cluster $[Zr_6O_4OH_4(COO)_{12}]$ fully coordinated by twelve carboxylates has O_h symmetry, which has many high-symmetry subgroups. This means that it is possible to decrease the connectivity and symmetry of Zr_6 to make it compatible with almost all kinds of organic linkers and form three-dimensional (3D) periodic frameworks. As almost all the Zr-MOFs contain the Zr_6 cluster, tuning the symmetry and connectivity of the Zr_6 cluster into a suitable node in a zeolite net would be an ideal approach to develop zeotype mesoporous MOFs.

Considering that the $[M_3O(COO)_6]$ unit in MIL-100 and MIL-101 has D_{3h} symmetry, a direct way to make zeotype Zr-MOFs is to lower the connectivity and symmetry of Zr_6 to D_{3h} while using the same organic linker. However, as D_{3h} symmetry is not a subgroup of O_h symmetry, it is not possible to obtain the same **mtn** network with Zr_6 when using only one type of organic linker. Fortunately, the major factor resulting in the formation of diverse zeolite structures is the variation of relative positions between adjacent tetrahedral nodes, and the $[M_3O(COO)_6]$ unit with D_{3h} symmetry in MIL-100 and MIL-101 only determines the eclipsed configuration between adjacent super-tetrahedra to generate the **mtn** network (Figure 1 a). When making a 60° rotation between each super-tetrahedron to form a staggered configuration, a β-cristobalite network can be constructed, which requires a six-connected D_{3d} node (Figure 1 b). Coincidently, D_{3d} is a subgroup of O_h symmetry, showing the theoretical feasibility of using the Zr_6 unit to build zeotype frameworks.

Topologically, both ditopic linear organic linkers and tritopic trigonal-planar organic linkers can form super-tetrahedra with six-connected D_{3d}-symmetric Zr_6 clusters of antiprismatic configuration. Linear organic linkers could serve as the edge while the trigonal-planar organic linkers could be the face. However, the challenge is to guarantee the formation of the Zr_6 unit with reduced connectivity as well as the correct symmetry to form the expected structures. With ditopic linear organic linkers, the Zr_6 cluster can form a **fcu-a** network with a twelve-connected O_h node, a **bcu-a** network with an eight-connected D_{4h} node, an **hxg-a** network with a six-connected hexagonal D_{3d} node, and a β-cristobalite network with six-connected antiprismatic D_{3d} node. Although these frameworks are topologically different, the other three are actually the subnetworks of the twelve-connected **fcu-a** network, which means that they can be obtained by simply decreasing the connecting linkers in the **fcu-a** network. Therefore, it is challenging to control the specific connectivity and symmetry without controlling the inherent kinetic or thermodynamic preference. All efforts to use higher zirconium to organic-linker ratios and more competing reagents to realize connectivity elimination have resulted in the formation of the **fcu-a** network with defects.[9]
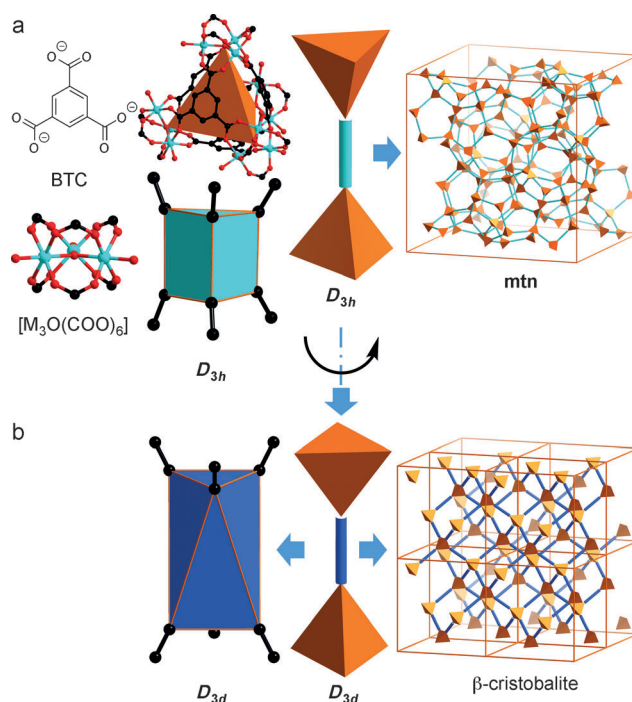

Figure 1. a) Inorganic and organic building units and symmetry analysis in the **mtn** type MOF MIL-100. The light-blue bar denotes an eclipsed configuration between adjacent tetrahedra with D_{3h}-connected nodes. b) Super-tetrahedral rotation from the **mtn** network to the β-cristobalite network. The dark-blue bar denotes a staggered configuration between adjacent tetrahedra with D_{3d}-connected nodes. BTC = benzene-1,3,5-tricarboxylate.

In comparison, trigonal planar organic linkers with three carboxylates in the same plane, which can form super-tetrahedra with six-connected antiprismatic D_{3d} Zr_6 clusters, can topologically form only one type of edge-transitive binodal network—the β-cristobalite-type network. Zr_6 clusters with all other reported connectivities and symmetries, such as twelve-connected O_h, eight-connected D_{4h}, and six-connected hexagonal D_{3d}, are not compatible with the formation of binodal edge-transitive networks with trigonal-planar organic linkers. Therefore, it is more likely to obtain mesoporous Zr-MOFs with a β-cristobalite network with trigonal-planar organic linkers.

Bearing such structural rationalization in mind, we selected a relatively large 4,4′,4″-s-triazine-2,4,6-triyl-tri-benzoate (TATB) linker, which prefers the trigonal-planar configuration, to construct the proposed Zr-MOF. To afford a partially substituted Zr_6 cluster we used excess Zr starting materials as well as trifluoroacetic acid (TFA) as a strong competing reagent. Solvothermal reaction between TATB, $ZrOCl_2 \cdot 8H_2O$, N,N-diethylformamide (DEF), and TFA gave rise to the formation of the product PCN-77 as a white powder (see the Supporting Information, section 3).

Synchrotron powder X-ray diffraction (PXRD) collected at 17-BM beamline at Advanced Photon Source, Argonne National Laboratory, shows that PCN-777 is cubic with unit-cell length a approximately 55 Å. This was further confirmed by 3D rotation electron diffraction (RED)[10] (Figure 2 a–c
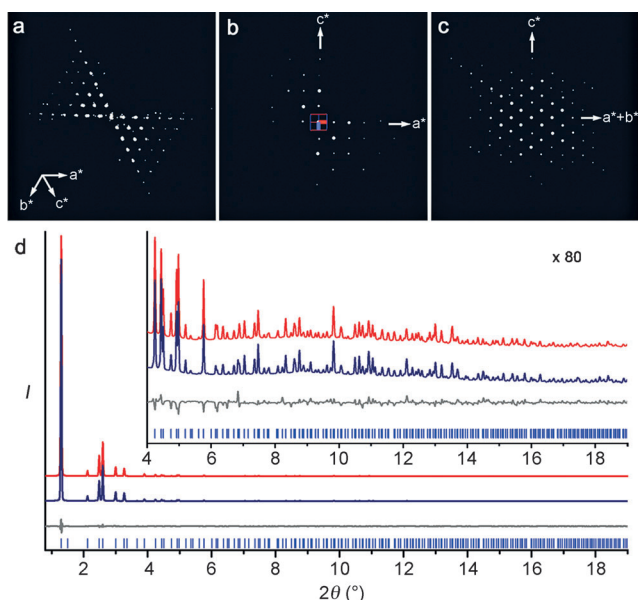
Figure 2. a) 3D reciprocal lattice of PCN-777 reconstructed from the RED data. b, c) 2D slices cut from the reconstructed 3D reciprocal lattice showing the b) *h*0 L and c) *hhl* plane. d) Rietveld refinement of PCN-777 using synchrotron PXRD data. The spectra from top to bottom are simulated (red), detected (blue), and difference profiles (grey), respectively; the bars below the curves indicate peak positions. Inset in (d): 80-fold magnification of the plots.

and the Supporting Information section 4). The reflection conditions deduced from the RED data gave the following five possible space groups: *F*23, *Fm*-3, *F*432, *F*-43*m*, and *Fm*-3*m*. Considering that the ideal space group of β-cristobalite is *Fd*-3*m*, the space group *F*-43*m*, which is the subspace group of *Fd*-3*m*, was chosen for the further structural study. A structural model of PCN-777, with a formula of $[Zr_6(O)_4(OH)_{10}(H_2O)_6(TATB)_2]$, was built based on our proposed β-cristobalite network using Material Studio 6.0[11] and further refined against the synchrotron PXRD data. Rietveld refinement with soft restraints for the M−O bond distances and a rigid body for the ligands shows a precise match between the experimental PXRD data and that simulated from the proposed structure (Figure 2 d).

The excess zirconium helps to form a six-connected D_{3d} Zr_6 building block, while the remaining coordinating positions are occupied by terminal OH and H_2O moieties. Unlike the D_{3d}-symmetric Zr_6 unit in PCN-224,[7g] the positions of the carboxylates and terminal OH/H_2O are switched to form an antiprismatic connecting mode in PCN-777. The overall structure of PCN-777 is built by sharing the vertexes of the super-tetrahedra, which consists of four Zr_6 units linked along the faces by the organic linkers (Figure 3 a). The organic linker TATB is almost twice the size of BTC (benzene-1,3,5-tricarboxylate), which makes the size of the super-tetrahedra in TATB-containing PCN-777 twice as large as those in MIL-100. Consequently, a mesoporous cage of 38 Å is formed in PCN-777, which is the largest pore among all reported Zr-MOFs. As a result of the high concentration of such mesoporous cages, the calculated porosity of PCN-777 reaches 3.38 cm³ g⁻¹. As expected, the D_{3d}-symmetric
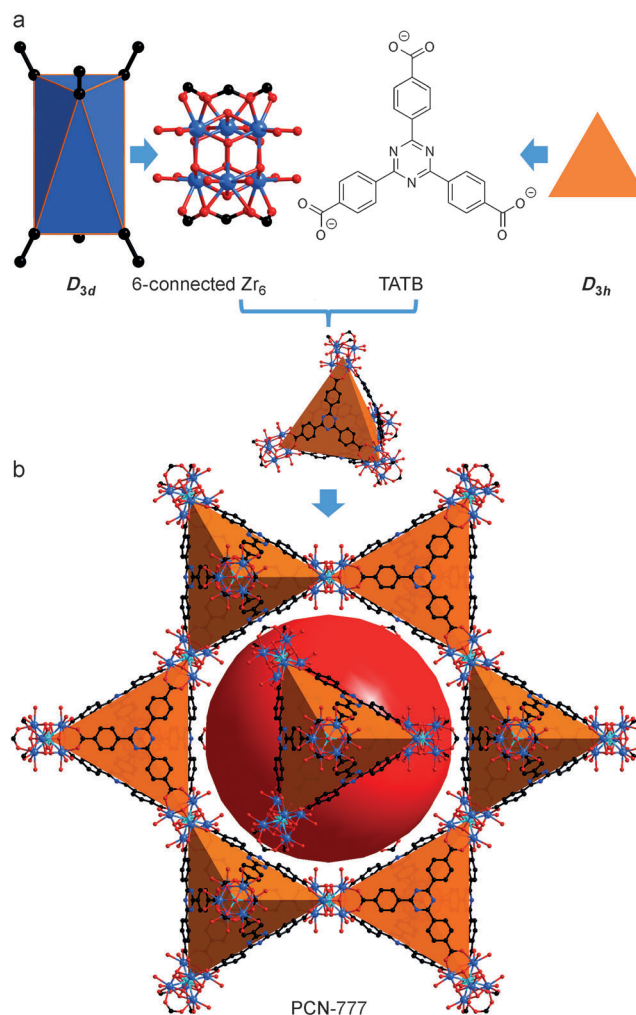

Figure 3. a) Six-connected D_{3d}-symmetric Zr_6 antiprismatic units and trigonal-planar organic linker TATB. b) The structure of PCN-777 with the large mesoporous cage (given in red).

Zr_6 cluster results in the formation of a perfectly staggered configuration of adjacent super-tetrahedra instead of the eclipsed configuration in MIL-100. The overall topology of PCN-777 changes from the **mtn** topology in MIL-100 to β-cristobalite type.

Owing to the relatively small ligand size and strong coordination bond between the organic linker and metal struts, PCN-777 can be activated directly upon the removal of solvent, while many other MOFs with such large pores and high porosity must be carefully activated with supercritical CO_2.[12] To assess the porosity of PCN-777, we performed N_2 sorption at 77 K (Figure 4 a). PCN-777 shows N_2 uptake of around 1460 cm³ g⁻¹ at 1 bar (Figure 4 a). The experimental Brunauer–Emmett–Teller (BET) surface area of PCN-777 is 2008 m² g⁻¹. A steep increase at $p/p_0 = 0.4$ on the N_2 adsorption isotherm corresponds to a mesoporous cage of 3.5 nm in PCN-777 (Figure 4 a, inset). The experimental void volume of PCN-777 is 2.82 cm³ g⁻¹, which is the highest among all the reported Zr-MOFs (see Table S2 in the Supporting Information).
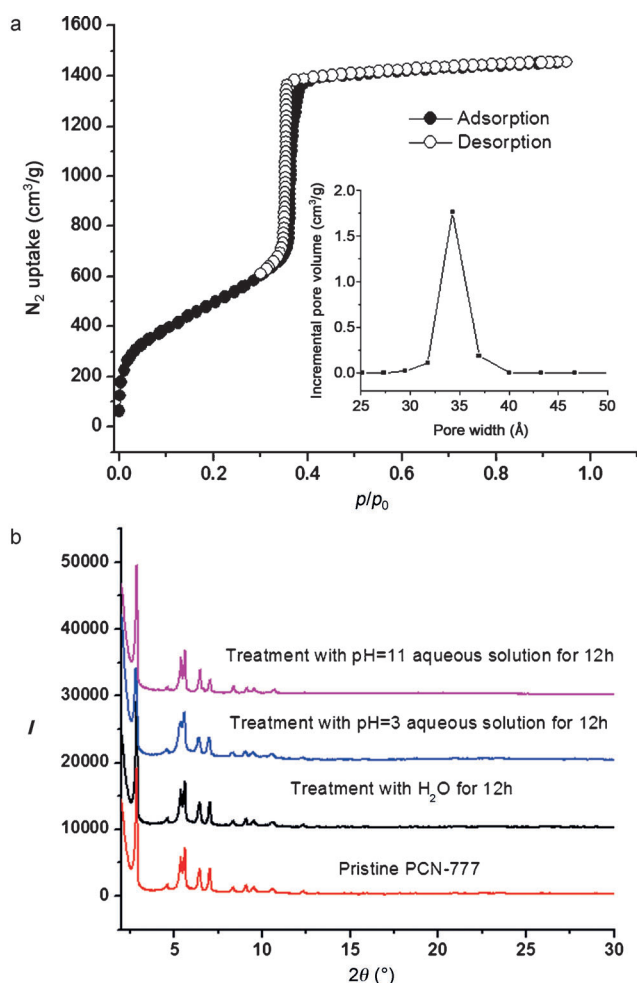
Figure 4. a) N_2 sorption isotherm of PCN-777. b) PXRD patterns of PCN-777 after different treatments.

Remarkably, PCN-777 has very high stability in aqueous solutions despite its high porosity. After soaking in distilled water and in aqueous solutions with pH = 3 and 11, PXRD patterns of PCN-777 are well maintained (Figure 4b). N_2 adsorption isotherms of these samples after the different treatments confirms the excellent stability of PCN-777 in pure H_2O and the basic environment while showing relatively weak stability in the acidic environment (Figure S2). The high positive charge density ($Z/r =$ charge/radius) on Zr^{IV} causes a strong electrostatic interaction between the metal nodes and ligand carboxylates, which endows the frameworks with excellent stability towards attack by reactive species. Thermal gravimetric analysis (TGA) indicates that the decomposition temperature of PCN-777 is around 500 °C (Figure S4), showing that the framework has very high thermal stability. The TGA curve also indicates that there are few or no missing-linker defects in the structure (see the Supporting Information, section 6).[13]

As a mesoporous MOF with very large pores and excellent chemical stability, PCN-777 is a suitable candidate to incorporate functional moieties with relatively large size through postsynthetic modification.[14] There are three major approaches to introduce functional moieties into MOFs:

direct physisorption, ionic trapping (in ionic MOFs), and covalent attachment through the functional anchors. As the Zr_6 cluster is only partially occupied by organic linkers, there are still positions available that can be functionalized for further modification. On one hand, the terminal OH/ H_2O groups can interact strongly with guests through either hydrogen or coordination bonding after deprotonation.[15] On the other hand, after one-step treatment, the terminal OH and H_2O on the Zr_6 cluster can be easily substituted by other carboxylate-containing species under very mild conditions, which is a convenient method to introduce many kinds of anchors.[16] Moreover, there are only six carboxylates coordinating to the Zr_6 cluster in PCN-777 and the empty positions are all pointing into the mesoporous cages. Therefore, the properties of the internal surface of the mesoporous cages in PCN-777 can be easily adjusted for further applications.

In fact, the trapping and leaching of guests in porous materials can be considered as equilibrium processes. When trapped guests are heterogeneously used, leaching becomes an entropically favored process. Therefore, to effectively prevent or diminish the leaching process, trapping guests inside the pores should be a highly enthalpically favored process, which requires strong interaction between the guests and supports.

Covalent attachment of guests can be thought of as an extreme method to enhance the trapping enthalpy. However, this approach always requires additional anchors on both the MOF framework and the incoming guests, which requires extra synthetic effort. In comparison, physical adsorption can directly incorporate guests. Although the interaction is usually weak, when the substrate is relatively large and multiple interacting sites could be provided by the framework, the overall interaction can still be strong enough to effectively prevent the substrate leaching. Accordingly, by postsynthetic modification of the internal surface, we examined the adsorption and leaching of different guests inside PCN-777. Using 4-*tert*-butylbenzoic acid (denoted as *t*Bu) and 4-carboxy-1-methylpyridinium iodide (denoted as Me-Py), we altered the internal surface from having the originally hydrophilic properties into being either highly hydrophobic or ionic. Three guests, *meso*-tetra(4-sulfonatophenyl)-porphyrin (TSPP), tris(2,2′-bipyridine) dichlororuthenium(II) ([Ru(bpy)$_3$]Cl$_2$), and tetra-amido macrocyclic ligand catalytic activators (TAML-NaFeB*, a catalyst for C−H bond activation; see Supporting Information, section 7), all of which having relatively large sizes but different functionalities, were incorporated into the modified PCN-777 (Figure 5). TSPP, as a porphyrinic derivative, can serve as a catalyst for different reactions and light-harvesting species. It shows the highest loading amount and slowest leaching in the pristine PCN-777 because of hydrogen bonding between the peripheral sulfonic groups and terminal OH/H_2O functionalities on the Zr_6 cluster. The system containing the anionic TAML-NaFeB* (the major part) shows the highest volumetric loading amount in Me-Py-modified PCN-777 despite having the lowest porosity because of the strong electrostatic interaction. In contrast, for [Ru(bpy)$_3$]Cl$_2$, a light harvesting reagent as well as a photocatalyst, there is no preferential loading in any framework as the functional part is cationic. As

Figure 5. Color variation of pristine, *t*Bu-modified, and Me-py-modified PCN-777 when loaded with different guests (TSPP, [Ru(bpy)₃]Cl₂, or TAML-NaFeB*).

expected, the *t*Bu-modified PCN-777 shows the weakest interaction with both TSPP and TAML-NaFeB* loadings because of the primarily nonpolar feature of the internal pore surface. We further test the catalytic activity of those trapped species in the postsynthetically modified PCN-777 species (see Supporting Information, section 8).

In conclusion, we designed and synthesized a zeotype mesoporous Zr-MOF, PCN-777. PCN-777 exhibits cages as large as 3.8 nm and excellent stability in aqueous environments, which make it an ideal candidate as a support to incorporate different functional moieties. Through facile internal pore surface modification, we can vary the interaction between PCN-777 and different guests to realize efficient immobilization.

Experimental Section

Synthesis of PCN-777: ZrOCl₂.8H₂O (360 mg), TATB (90 mg), and trifluoroacetic acid (0.6 mL) in DEF (12 mL) were ultrasonically dissolved in a 20 mL Pyrex vial. The mixture was heated at 120 °C in an oven for 12 h. After cooling to room temperature, a white powder product of PCN-777 was collected by filtration.

Crystal data from PXRD of PCN-777: $Zr_6O_{122}C_{48}N_6H_{24}$, $M = 3184.05$, space group *F-43 m*, $a = 55.568(3)$ Å, $V = 171583(5)$ Å³, $Z = 16$, total reflections = 514, GOF = 1.134, $R_p = 0.0395$, $R_{wp} = 0.0564$, $R_{exp} = 0.0497$ (see the Supporting Information, section 4).

CCDC-1013322 (PCN-777) contains the supplementary crystallographic data for this paper. This data can be obtained free of charge from The Cambridge Crystallographic Data Centre via www.ccdc.cam.ac.uk/data_request/cif.

Full experimental details can be found in the Supporting Information.

[1] H.-C. Zhou, J. R. Long, O. M. Yaghi, *Chem. Rev.* **2012**, *112*, 673–674.

[2] a) Q.-L. Zhu, Q. Xu, *Chem. Soc. Rev.* **2014**, *43*, 5468–5512; b) H. Deng, S. Grunder, K. E. Cordova, C. Valente, H. Furukawa, M. Hmadeh, F. Gándara, A. C. Whalley, Z. Liu, S. Asahina, H. Kazumori, M. O'Keeffe, O. Terasaki, J. F. Stoddart, O. M. Yaghi, *Science* **2012**, *336*, 1018–1023; c) Y. K. Hwang, D. Y. Hong, J. S. Chang, S. H. Jhung, Y. K. Seo, J. Kim, A. Vimont, M. Daturi, C. Serre, G. Férey, *Angew. Chem. Int. Ed.* **2008**, *47*, 4144–4148; *Angew. Chem.* **2008**, *120*, 4212–4216; d) Y. Chen, V. Lykourinou, C. Vetromile, T. Hoang, L.-J. Ming, R. W. Larsen, S. Ma, *J. Am. Chem. Soc.* **2012**, *134*, 13188–13191.

[3] a) V. Guillerm, F. Ragon, M. Dan-Hardi, T. Devic, M. Vishnuvarthan, B. Campo, A. Vimont, G. Clet, Q. Yang, G. Maurin, G. Ferey, A. Vittadini, S. Gross, C. Serre, *Angew. Chem. Int. Ed.* **2012**, *51*, 9267–9271; *Angew. Chem.* **2012**, *124*, 9401–9405; b) T. Devic, C. Serre, *Chem. Soc. Rev.* **2014**, *43*, 6097–6115.

[4] a) G. Férey, C. Mellot-Draznieks, C. Serre, F. Millange, J. Dutour, S. Surblé, I. Margiolaki, *Science* **2005**, *309*, 2040–2042; b) G. Férey, C. Serre, C. Mellot-Draznieks, F. Millange, S. Surblé, J. Dutour, I. Margiolaki, *Angew. Chem. Int. Ed.* **2004**, *43*, 6296–6301; *Angew. Chem.* **2004**, *116*, 6456–6461.

[5] a) M. Li, D. Li, M. O'Keeffe, O. M. Yaghi, *Chem. Rev.* **2014**, *114*, 1343–1370; b) http://rcsr.anu.edu.au/.

[6] a) P. Horcajada, S. Surble, C. Serre, D.-Y. Hong, Y.-K. Seo, J.-S. Chang, J.-M. Greneche, I. Margiolaki, G. Férey, *Chem. Commun.* **2007**, 2820–2822; b) C. Volkringer, D. Popov, T. Loiseau, G. Ferey, M. Burghammer, C. Riekel, M. Haouas, F. Taulelle, *Chem. Mater.* **2009**, *21*, 5695–5697; c) A. Lieb, H. Leclerc, T. Devic, C. Serre, I. Margiolaki, F. Mahjoubi, J. S. Lee, A. Vimont, M. Daturi, J.-S. Chang, *Microporous Mesoporous Mater.* **2012**, *157*, 18–23; d) S. Surblé, C. Serre, C. Mellot-Draznieks, F. Millange, G. Férey, *Chem. Commun.* **2006**, 284–286.

[7] a) J. H. Cavka, S. Jakobsen, U. Olsbye, N. Guillou, C. Lamberti, S. Bordiga, K. P. Lillerud, *J. Am. Chem. Soc.* **2008**, *130*, 13850–13851; b) C. Wang, J.-L. Wang, W. Lin, *J. Am. Chem. Soc.* **2012**, *134*, 19895–19908; c) C. Wang, Z. Xie, K. E. deKrafft, W. Lin, *J. Am. Chem. Soc.* **2011**, *133*, 13445–13454; d) H.-L. Jiang, D. Feng, J.-R. Li, T.-F. Liu, H.-C. Zhou, *J. Am. Chem. Soc.* **2012**, *134*, 14690–14693; e) D. Feng, Z. Y. Gu, J. R. Li, H. L. Jiang, Z. Wei, H. C. Zhou, *Angew. Chem. Int. Ed.* **2012**, *51*, 10307–10310; *Angew. Chem.* **2012**, *124*, 10453–10456; f) W. Morris, B. Volosskiy, S. Demir, F. Gándara, P. L. McGrier, H. Furukawa, D. Cascio, J. F. Stoddart, O. M. Yaghi, *Inorg. Chem.* **2012**, *51*, 6443–6445; g) D. Feng, W.-C. Chung, Z. Wei, Z.-Y. Gu, H.-L. Jiang, Y.-P. Chen, D. Darensbourg, H.-C. Zhou, *J. Am. Chem. Soc.* **2013**, *135*, 17105–17110; h) J. E. Mondloch, W. Bury, D. Fairen-Jimenez, S. Kwon, E. J. DeMarco, M. H. Weston, A. A. Sarjeant, S. T. Nguyen, P. C. Stair, R. Q. Snurr, O. K. Farha, J. T. Hupp, *J. Am. Chem. Soc.* **2013**, *135*, 10294–10297; i) H. Furukawa, F. Gándara, Y.-B. Zhang, J. Jiang, W. L. Queen, M. R. Hudson, O. M. Yaghi, *J. Am. Chem. Soc.* **2014**, *136*, 4369–4381; j) M. Kim, J. F. Cahill, H. Fei, K. A. Prather, S. M. Cohen, *J. Am. Chem. Soc.* **2012**, *134*, 18082–18088; k) S. Pullen, H. Fei, A. Orthaber, S. M. Cohen, S. Ott, *J. Am. Chem. Soc.* **2013**, *135*, 16997–17003; l) H. Fei, S. M. Cohen, *Chem. Commun.* **2014**, *50*, 4810–4812; m) M. Kim, S. M. Cohen, *CrystEngComm* **2012**, *14*, 4096–4104.

[8] A. Schaate, P. Roy, A. Godt, J. Lippke, F. Waltz, M. Wiebcke, P. Behrens, *Chem. Eur. J.* **2011**, *17*, 6643–6651.

[9] a) H. Wu, Y. S. Chua, V. Krungleviciute, M. Tyagi, P. Chen, T. Yildirim, W. Zhou, *J. Am. Chem. Soc.* **2013**, *135*, 10525–10532; b) F. Vermoortele, B. Bueken, G. Le Bars, B. Van de Voorde, M. Vandichel, K. Houthoofd, A. Vimont, M. Daturi, M. Waroquier, V. Van Speybroeck, C. Kirschhock, D. E. DeVos, *J. Am. Chem. Soc.* **2013**, *135*, 11465–11468.

[10] a) D. L. Zhang, S. Hovmöller, P. Oleynikov, X. Zou, *Z. Kristallogr.* **2010**, *225*, 94–102; b) W. Wan, J. L. Sun, J. Su, S. Hovmöller, X. Zou, *J. Appl. Crystallogr.* **2013**, *46*, 1863–1873.

[11] Accelerys Materials Studio Release Notes, Release 5.5.1; Accelerys. Software, Inc.: San Diego, **2010**.

[12] a) T. Li, M. T. Kozlowski, E. A. Doud, M. N. Blakely, N. L. Rosi, *J. Am. Chem. Soc.* **2013**, *135*, 11688–11691; b) O. K. Farha, I. Eryazici, N. C. Jeong, B. G. Hauser, C. E. Wilmer, A. A. Sarjeant, R. Q. Snurr, S. T. Nguyen, A. O. Yazaydin, J. T. Hupp, *J. Am. Chem. Soc.* **2012**, *134*, 15016–15021.

[13] a) G. C. Shearer, S. Chavan, J. Ethiraj, J. G. Vitillo, S. Svelle, U. Olsbye, C. Lamberti, S. Bordiga, K. P. Lillerud, *Top Catal* **2013**,

56, 770–782; b) G. C. Shearer, S. Chavan, J. Ethiraj, J. G. Vitillo, S. Svelle, U. Olsbye, C. Lamberti, S. Bordiga, K. P. Lillerud, *Chem. Mater.* **2014**, *26*, 4068–4071.

[14] a) S. M. Cohen, *Chem. Rev.* **2011**, *111*, 970–1000; b) K. K. Tanabe, S. M. Cohen, *Chem. Soc. Rev.* **2011**, *40*, 498–519.

[15] R. Ameloot, M. Aubrey, B. M. Wiers, A. P. Gomora-Figueroa, S. N. Patel, N. P. Balsara, J. R. Long, *Chem. Eur. J.* **2013**, *19*, 5533–5536.

[16] P. Deria, J. E. Mondloch, E. Tylianakis, P. Ghosh, W. Bury, R. Q. Snurr, J. T. Hupp, O. K. Farha, *J. Am. Chem. Soc.* **2013**, *135*, 16801–16804.
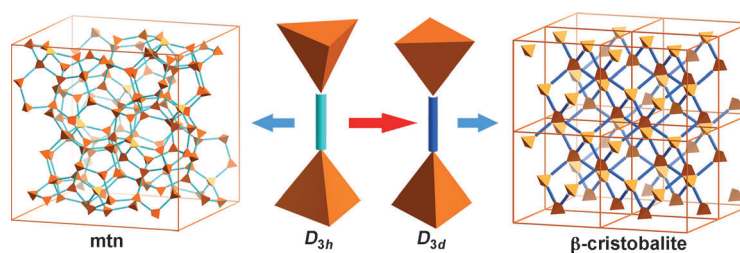
↖↖ These are not the final page numbers!

Communications

Metal–Organic Frameworks

D. Feng, K. Wang, J. Su, T.-F. Liu, J. Park,
Z. Wei, M. Bosch, A. Yakovenko, X. Zou,
H.-C. Zhou* ⬛⬛⬛⬛–⬛⬛⬛⬛

A Highly Stable Zeotype Mesoporous
Zirconium Metal–Organic Framework
with Ultralarge Pores

mtn D_{3h} D_{3d} β-cristobalite

Topological rationalization is used to design a zeotype mesoporous Zr metal–organic framework. When tetrahedra (orange; see picture) with $[M_3O(COO)_6]$ nodes and tridentate benzene-1,3,5-tricarboxylate faces are connected in an eclipsed configuration (D_{3h} nodes; light-blue bar), an mtn network is formed. A 60° rotation between tetrahedra gives a staggered configuration with D_{3d}-connected nodes (dark-blue bar) and a β-cristobalite network.